Journal of Non-Crystalline Solids 354 (2008) 4151–4156

Contents lists available at ScienceDirect

Journal of Non-Crystalline Solids

journal homepage: www.elsevier.com/locate/jnoncrysol

Uncertainty modeling of carbon nanotube terahertz oscillators

F. Scarpa [a,*], S. Adhikari [b]

[a] Department of Aerospace Engineering, University of Bristol, Bristol BS8 1TR, UK
[b] School of Engineering, University of Wales, Swansea SA2 8PP, UK

ARTICLE INFO

Article history:
Available online 4 August 2008

PACS:
62.25.Fg
62.25.Jk
64.40.De

Keyword:
Mechanical properties

ABSTRACT

Significant uncertainties have been reported in the material properties of carbon nanotubes. In this paper, a probabilistic approach to take account of these uncertainties is proposed. The probability density function of the natural frequencies is derived in closed-form. The new results are compared with high-fidelity stochastic finite element simulations.

1. Introduction

Recently, single wall carbon nanotubes (SWCNTs) have been proposed as THz oscillators for novel applications as NEMS (Nano Electro-Mechanical Systems), high-frequency filters for wireless systems and bio-sensors [1]. The rationale behind the use of nanostructures as high-end resonators is their low mass, low force constant and high resonant frequencies. As bio-sensors, nanostructures-based designs have shown the capability of weighing single bacteria [2] and detecting single spins in magnetic resonance devices [3]. Numerical simulations using a structural-molecular mechanics method have shown great potential on using SWCNTs as nanobalances with mass sensitivity of 10^{-21} g and analogous sensitivity of resonant frequency shifts to both tube length and radius [4] (Fig. 1).

For sensor design, it is important to handle data related to the multiphysics material characteristics with known and reliable statistical properties. In this way, design iteration and sensitivity analysis can be performed with sufficient confidence to provide at the end a reliable product, as much as the current technological landscape allows. This is also true for nanoelectromechanical systems (NEMS), considering also the increasing interest that these devices attract also in the market place. However, experimental mechanical data related to SWCNTs and multiwalled carbon nanotubes (MWCNTs) feature significant scatter. Salvetat et al. [5] measured the flexural Young's modulus and shear modulus using AFM test on clamped–clamped nanoropes, obtaining values with 50% of error. Information related to statistical distributions of experimental data is also scarce, and the important paper from Krishnan et al. [6] provides one of the few examples available of histogram distribution of the flexural Young's modulus derived from 27 CNTs. The Young's modulus was obtained observing free-standing vibrations at room temperature using transmission electro-microscope (TEM), with a mean value of 1.3 TPa -0.4 TPa/+0.6 TPa. Notably, in [6], stochastically averaged probability amplitude for the vibration modes is calculated to obtain the rms vibration profile along the length of the tubes.

The importance of the scatter of experimental data from single production batches of nanotubes during free-standing vibration is also evinced from [7]. The first bending mode frequency ranges from 0.64 MHz to 1.42 MHz. Moreover, the carbon nanostructures feature significant weaviness – a factor that induces important changes in the natural frequencies of slender structures [8]. Extensive scatter of Q^{-1} factors has been also recently recorded for novel nanosensor devices based on bridged-bridges MWCNTs [3].

Uncertainty is also associated to the equivalent atomistic-continuum models used extensively during the last years, in particular by the engineering and materials science communities. A global review of the most used methods can be found in [9]. With the equivalent atomistic-continuum models, the equivalence between the chemical potential and mechanical strain energy of the structural components which are assumed constitute the truss-like structure of the carbon nanotube is imposed, allowing to identify also the thickness of the carbon nanostructures. However, in the seminal paper from Huang et al. [10], the extensive scatter of thickness values from different models existing in open literature, ranging from 0.06 nm to 0.69 nm. In [10], a closed-form solution for the thickness of graphene sheet based on Brenner potentials and equivalent with Kirschoff's plate theory was derived under different loading

* Corresponding author. Tel.: +44 117 92 89861; fax: +44 117 92 72771.
E-mail addresses: f.scarpa@bris.ac.uk, scarpa.fabrizio@gmail.com (F. Scarpa).

0022-3093/$ - see front matter © 2008 Elsevier B.V. All rights reserved.
doi:10.1016/j.jnoncrysol.2008.06.065

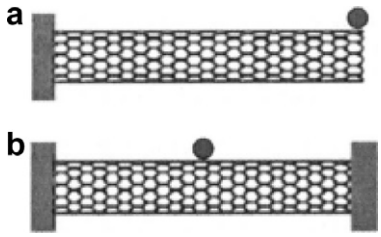

Fig. 1. Nanotube resonator with attached mass: (a) clamped-free; (b) bridged (from [14]).

conditions, and considerations for the thickness of carbon nanoropes were also made. An important outcome of the investigation in [10] was the dependence of the thickness values on the CNT radius and type of loading. Yet, the thickness has to be used to calculate the inertia properties of the beams in order to extract the flexural modulus from the experimental data. The complex relation between thickness and loading, as well as the uncertainty associated with the experimental setup makes the use of continuum models for the deterministic design of nanodevices a difficult task.

The stochastic modeling on the carrier dynamics in nanostructures has been recently proposed by Barzykin and Tachiya [11]. However, to the Authors' knowledge, a model to capture the uncertainty and stochastics of SWCNTs in bending vibration for high-frequency oscillations has not been proposed so far. Yet, the knowledge of the sensitivity of the different nanooscillator designs against mechanical parameters or environmental noise would be beneficial, as been observed recently for nanotube transistors in detection of noisy subthreshold signals [12].

In this work, we proposed a stochastic reduced order model of the natural frequencies for a SWCNT to take into account the uncertainty of the equivalent mechanical associated to the continuum model. The SWCNT is modeled as a Euler–Bernoulli beam [13], with no cross-section shear deformation allowed. The dependence of the natural frequencies versus the probability density functions (pdfs) of the mechanical parameters (flexural modulus and mass per unit length) is derived in a closed-form solution. Because of lack of sufficient data from open literature regarding experimental pdfs of flexural modulus, an equivalent atomistic-continuum Finite Element model proposed by Tserpes and Papanikos [14] has been used to generate statistical data of the flexural modulus. Considering also the uncertainty associated with the thickness scattering, the mass per unit length has been also considered a random variable in this work. The pdfs of the mechanical parameters have been generated with a direct Monte Carlo (MC) method, and fed back to the analytical model developed. The natural frequencies calculated form the analytical models have been compared with the ones calculated from the FE (finite element) model, providing good agreement.

2. Dynamics with reduced continuous Euler–Bernoulli beam model with uncertainty

The natural frequencies of a SWCNT modeled as an Euler–Bernoulli beam can be expressed as

$$\omega_n = c_n\sqrt{\frac{E_f I}{mL^4}}; \quad n = 1,2,\ldots, \tag{1}$$

where c_n are coefficients depending on the boundary conditions [13], E_f is the flexural modulus of the beam material and I the inertia moment of the beam. The flexural stiffness of the beam is represented by $E_f I$, while m is the mass per unit length and L is the length of the carbon nanotube. Based on the information regarding the uncertainty of the parameters, we can consider the case where both the flexural stiffness and the mass distribution could be assumed to be jointly random, with some specific correlation. For convenience, we express Eq. (1) as

$$u = \bar{c}_n\sqrt{\frac{x}{y}} = \bar{c}_n\sqrt{z}, \tag{2}$$

where the constant $\bar{c}_n = c_n = L^2$ and the random variables $x = E_f I$, $y = m$, $u = \omega_n$ and $z = x/y$. Suppose the joint probability density function of x and y is given by $p_{xy}(x;y)$. Following Papoulis and Pillai [15, Chapter 6], the probability density function of z can be regarded as

$$p_z(z) = \int_0^\infty y p_{xy}(yz,y)\mathrm{d}y + \int_0^\infty y p_{xy}(-yz,-y)\mathrm{d}y \tag{3}$$

We consider that $E_f I$ and m are jointly Gaussian random variable with correlation coefficient r. Their joint probability density function is given by

$$p_{xy}(x,y) \equiv p_{\mathbf{X}}(\mathbf{x}) = \frac{1}{2\pi|\mathbf{\Sigma}|^{1/2}}\exp\left\{-\frac{1}{2}(\mathbf{x}-\mathbf{m})^{\mathrm{T}}\mathbf{\Sigma}^{-1}(\mathbf{x}-\mathbf{m})\right\}, \tag{4}$$

where

$$\mathbf{x} = \begin{Bmatrix} x \\ y \end{Bmatrix}; \quad \mathbf{m} = \begin{Bmatrix} m_1 \\ m_2 \end{Bmatrix}; \quad \mathbf{\Sigma} = \begin{bmatrix} \sigma_1^2 & r\sigma_1\sigma_2 \\ r\sigma_1\sigma_2 & \sigma_2^2 \end{bmatrix}. \tag{5}$$

In order to obtain $pxy(yz;y)$, we note that

$$x = \begin{Bmatrix} czy \\ y \end{Bmatrix} = y\begin{Bmatrix} cz \\ 1 \end{Bmatrix} = y\mathbf{v}(z); \quad \text{where } \mathbf{v}(z) = \begin{Bmatrix} cz \\ 1 \end{Bmatrix}. \tag{6}$$

Inserting (6) in (4) and evaluating the integral (3) (see Appendix A for details), one obtains:

$$p_z(z) = \alpha(z)\exp\{-\beta^2/2\}\left(1+\gamma(z)\sqrt{2\pi}(\Phi(\gamma(z))-1/2)\exp\{\gamma^2(z)/2\}\right), \tag{7}$$

where $\Phi(\cdot)$ is the cumulative normal distribution function and:

$$\alpha(z) = \frac{1}{\pi\mathbf{v}^{\mathrm{T}}(z)\mathbf{\Sigma}^{-1}\mathbf{v}(z)\sqrt{\det\mathbf{\Sigma}}}, \tag{8}$$

$$\gamma(z) = \frac{\mathbf{v}^{\mathrm{T}}(z)\mathbf{\Sigma}^{-1}\mathbf{m}}{\sqrt{\mathbf{v}^{\mathbf{T}}(\mathbf{z})\mathbf{\Sigma}^{-1}\mathbf{v}(\mathbf{z})}}, \tag{9}$$

$$\beta^2 = \mathbf{m}^{\mathrm{T}}\mathbf{\Sigma}^{-1}\mathbf{m}. \tag{10}$$

From the transformation (2), the probability density of the natural frequencies of the SWCNT can be expressed as

$$p_u(u) = \frac{2u}{\bar{c}_n^2}p_z(u^2/\bar{c}_n^2). \tag{11}$$

3. Finite element model

The finite element models of the SWCNT were based on the formulation proposed by Tserpes and Papanikos [14], using the commercial FE code ANSYS [16]. The models were constituted by BEAM4 and MASS21 elements, representing the C–C bonds and atom masses, respectively. The equivalent Young's modulus E, shear modulus G and diameter d of the C–C bonds were defined as [17]:

$$E = \frac{k_r^2 l}{4\pi k_\theta}, \tag{12}$$

$$G = \frac{k_r^2 k_\tau l}{8\pi k_\theta^2}, \tag{13}$$

$$d = 4\sqrt{\frac{k_\theta}{k_r}}, \tag{14}$$

where k_r and k_θ are respectively 6.52×10^{-7} N nm^{-1} and 8.76×10^{-10} N nm rad^{-2}. The value of $k_\tau = 2.78 \times 10^{-10}$-N nm rad^{-2} was adopted from the AMBER force model [18]. The length l of the C–C bonds is 0.1421 nm, while the mass m of the atoms is considered 1.9943×10^{-26} kg.

The bridged layout was simulated imposing a clamped–clamped (CC) boundary condition, restraining all the degrees of freedom to zero values. The SWCNTs were loaded at the center with a distribution of concentrated forces on the external nodes of the diameter of the central section. The equivalent flexural modulus of the carbon nanotube was calculated using the Engineering Beam Theory [19]:

$$E_f I = \frac{FL^3}{192\delta}, \tag{15}$$

where δ is the central deflection of the tube under loading F calculated after a linear static analysis. Assuming a hollow tube configuration for the SWCNT, the moment of inertia I can be evaluated using the following formula [14]:

$$I = \frac{1}{32}\left[(D+t)^4 - (D-t)^4\right], \tag{16}$$

where D is the mean diameter of the hollow tube, while t is the thickness (equivalent to the cross-section dimension d). Simulations related to a clamped-free condition (CF) were also carried out to discern some possible differences between the flexural modulus obtained by the two types of loading. In that case, the bending modulus in Eq. (15) would assume the value of $(FL^3/3\delta)$ [19].

The natural frequencies of the CC case were evaluated using a Subspace Iteration Technique using a 10 vectors subspace to extract the first four eigenvalues and eigenvectors. All the calculations were carried out on a 2.2 GHz single processor PC. No eigenvalue analysis was performed for the CF case.

The MC simulations were carried out considering a Gaussian distribution perturbation to the values of k_r, k_τ and k_θ to represent stochastic variations due to thermal oscillations, uncertainty of the thickness (via Eq. (14)), as well as uncertainty associated to the imperfections of the applied BCs. The Gaussian distributions had mean values corresponding to the standard cases are reported previously, and standard deviations corresponding to 12%, 13% and 15% of the mean values respectively for the equivalent bond force constants. Thousand samples were generated using a direct MC method where the force constants variables were considered

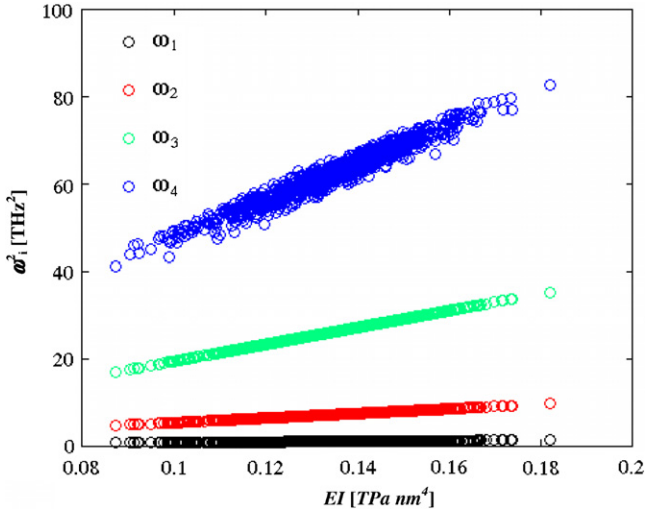

Fig. 4. FE simulated results for squared natural frequencies [THz^2] versus flexural bending stiffness [TPa nm^4].

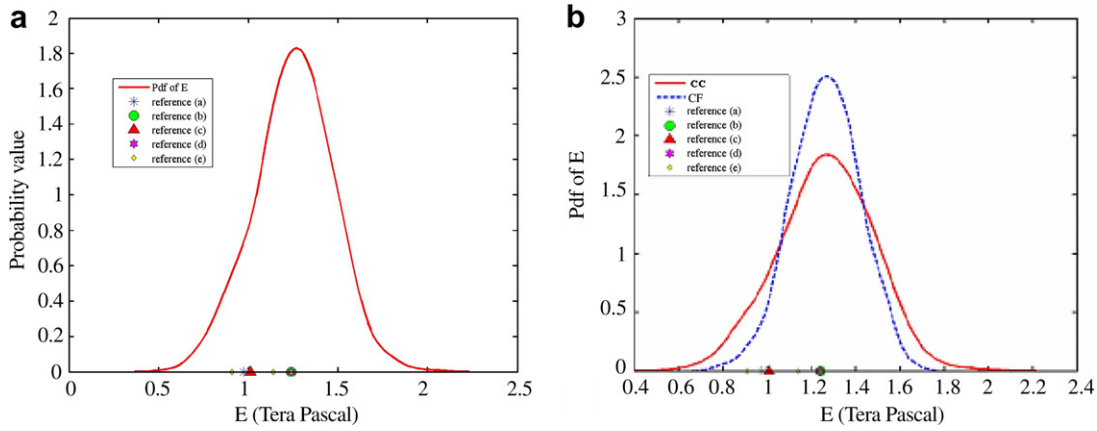

Fig. 2. Pdfs of the flexural modulus for the CC case (a) and CF cases (b). Comparison with experimental data. All figures – Ref. (a) [21], Ref. (b) [22], Ref. (c) [23], Ref. (d) [24], Ref. (e) [25].

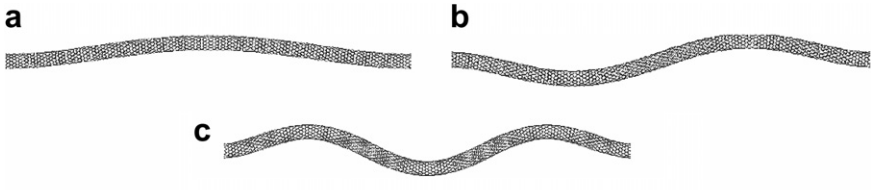

Fig. 3. First (a), second (b) and third (c) CC bending vibration modes an armchair (12,12) SWCNT.

uncorrelated. The analysis (static and modal) were carried out on a base configuration consisting on armchair tubule (12,12), with base diameter of 1.628 nm and length corresponding to 28.13 nm. The model had 1278 elements.

4. Results and discussion

The FE MC simulations provided a distribution of the flexural modulus after static loading, as per simulating an atomic force microscope (AFM) test on a clamped–clamped specimen [5]. The simulated flexural modulus distribution was then used to calculate the probability distributions of the natural frequencies via the analytical models. The natural frequencies calculated via the FE procedure were also used to identify the flexural modulus corresponding to the bending mode in consideration, similarly to the experimental procedure used to identify the Young's modulus via electric field emissions [20].

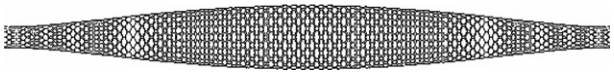

Fig. 5. First breathing mode.

Fig. 2(a) shows the pdfs of the flexural modulus of the SWCNT in the bridged case, as well as the experimental results of Young's modulus as reported by Lu [21], Hernández [22], Li and Chou [23], Jin and Yuane [24], and Qi et al. [25]. The mean value of the flexural Young's modulus from the FE based simulations is 1.25 TPa, well in agreement with the published data. As stated before, no similar consideration can be done for the probability distribution associated to the flexural modulus, because of lack of analogous comparison. Fig. 2(b) shows also the influence of the type of base BC conditions used for the loading case. The clamped-free (CF) boundary conditions were simulated leaving a free edge with no restraints, and applying a distribution of forces on the nodes of the end section. The analogous CF probability distribution for the flexural modulus provides a narrower curve around the same mean value of the CC case, with a smaller tail towards 0.6 TPa and 1.8 TPa compared to the bridged case. The assumption of the Euler–Bernoulli beam theory (pure bending modes for the slender beam) is satisfied for the first three modes of the SWCNT case considered, as shown in Fig. 3. Fig. 4 shows the first four squared natural frequencies versus the flexural stiff-

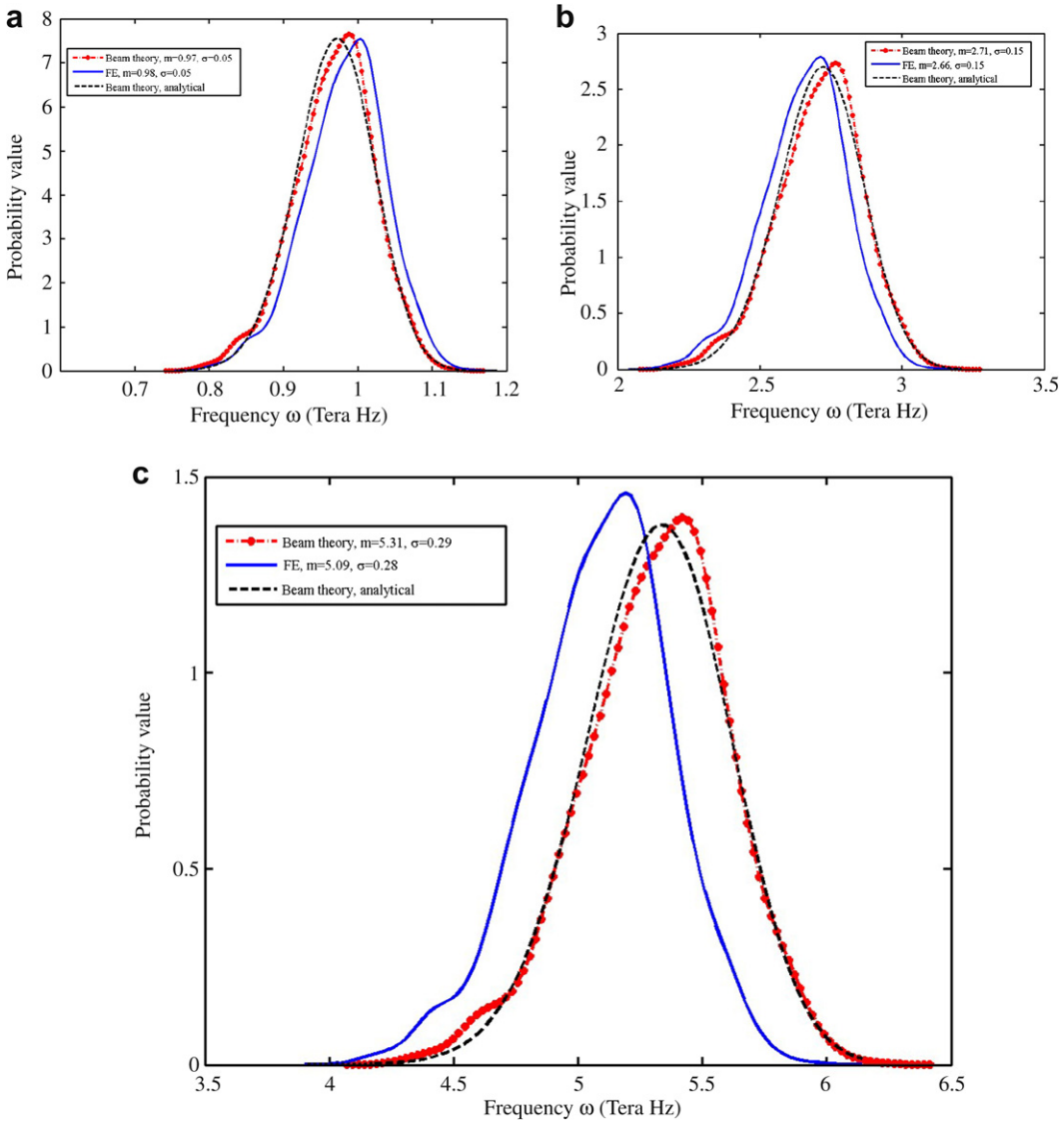

Fig. 6. Probability distributions for first (a), second (b) and third (c) natural frequencies of the SWCNT. Comparisons between analytical, FE and updated analytical models.

ness of the SWCNTs as simulated by the stochastic FE models. From Eq. (1) a linear dependency of w_i^2 versus EI would indicate a pure bending mode of the beam, while any departure from linearity would indicate vibration modes not consistent with the slender beam theory. The first three resonances of the SWCNT models behave all linearly, while the forth one indicates possible switches between 4th order bending modes and breathing modes (Fig. 5). Donnell–Vlasov theories would then be required to model accurately radial and membrane modes of the tubes [26], however for practical reasons oscillations between 1 GHz and 5 GHz are most required [2], and shell-type models would only offer accuracy for higher order modes. Fig. 6 shows the comparison between the analytical and FE simulated probability density functions of the first three bending modes of the SWCNTs. For the first bending mode (Fig. 6a), the discrepancy of the mean value between the analytical model with flexural modulus derived from the first FE mode and the full finite element simulation is about 1.4%, with an analogous standard deviation percentage error of 1.8%. Similar trends are recorded for the second mode in Fig. 6(b), with discrepancy in the mean value and standard deviation of 1.9% and 2.0%, respectively. For the third bending mode (Fig. 6(c)), the discrepancies are higher (4.3% and 3.6%, respectively), however still within a very satisfactory engineering comparison. For all the simulations, the analytical ones with the static flexural stiffness provide a close comparison with the analytical with flexural dynamic updated modulus. It must be also pointed out that the stochastic FE models take into account a general anisotropy of the mechanical behavior of the SWCNTs, with the axial stiffness on average being 3–4 times the flexural one [14,10,21]. The anisotropic behavior is not taken into account by the analytical Euler–Bernoulli beam model, where an isotropic material undergoing pure flexural deformation is considered. The probability density function distributions are also not symmetrical around the mean value, due to the different standard distributions attributed to the constants k_s, k_τ and k_θ in the FE-generated data. However, the different tails and non-symmetric distribution of the flexural modulus are consistent with the ones published in [5].

5. Conclusions

An analytical model providing the probability density functions of the natural frequencies of single wall carbon nanotube terahertz oscillators has been proposed. The model provides prediction of the stochastic properties of the resonances of the SWCNTs with known input of analogous pdfs related to the flexural modulus, the mass per unit length, or both, all in a closed-form solution. Due to lack of exhaustive information on experimental pdfs, stochastic distributions have been generated using a FE model based on atomistic-continuum equivalence. The agreement between the results from the analytical model and the finite element simulations is good. The analytical model proposed has been developed for design issues. However, the same model could be also used in principle to identify the type of uncertainty associated to experimental data when available. At the same time, it would be desirable also to improve the fidelity of numerically generated data by improving existing atomistic-continuum equivalent models using more MD simulations and improved force models.

Acknowledgement

Sondipon Adhikari acknowledges the support of the UK Engineering and Physical Sciences Research Council (EPSRC) through the award of an Advanced Research Fellowship, Grant No. GR/T03369/01. Fabrizio Scarpa acknowledges the contribution from the FP6 STRP01364 project CHISMACOMB for part of the CPU time.

Appendix A

A.1. Derivation of the PDF for the general case

Substituting Eq. (5) in (4) and simplifying one obtains:

$$p_{xy}(yz,y)=\frac{e^{-b^2/2}}{2\pi|\boldsymbol{\Sigma}|^{1/2}}\exp\left\{-\frac{(y-a)^2}{2\sigma^2}\right\}, \tag{A.1}$$

where

$$\sigma^2=\frac{1}{\mathbf{v}^{\mathrm{T}}\boldsymbol{\Sigma}^{-1}\mathbf{v}};\quad a=\frac{\mathbf{v}^{\mathrm{T}}\boldsymbol{\Sigma}^{-1}\mathbf{m}}{\mathbf{v}^{\mathrm{T}}\boldsymbol{\Sigma}^{-1}\mathbf{v}} \tag{A.2}$$

and

$$b^2=\mathbf{m}^{\mathrm{T}}\boldsymbol{\Sigma}^{-1}\mathbf{m}-\frac{a^2}{\sigma^2}. \tag{A.3}$$

Similarly one obtains

$$p_{xy}(-yz,-y)=\frac{e^{-b^2/2}}{2\pi|\boldsymbol{\Sigma}|^{1/2}}\exp\left\{-\frac{(y+a)^2}{2\sigma^2}\right\}. \tag{A.4}$$

Substituting (A.4) and (A.1) into Eq. (3) one obtains, after some manipulation:

$$p_z(z)=\frac{\exp\{-(b^2+a^2/\sigma^2)/2\}}{2\pi|\boldsymbol{\Sigma}|^{1/2}}\times\int_0^\infty\left[y\exp\{-\mu y^2-2\nu y\}+y\exp\{-\mu y^2+2\nu y\}\right]\mathrm{d}y, \tag{A.5}$$

where

$$\mu=\frac{1}{2\sigma^2};\quad \nu=\frac{a}{2\sigma^2}. \tag{A.6}$$

A closed-form solution of (A.5) can be obtained as [15, p. 361]:

$$p_z(z)=\frac{\exp-\{\beta^2/2\}}{2\pi|\Sigma|^{1/2}}\left[\begin{array}{l}\frac{1}{2\mu}-\frac{\nu}{2\mu}\sqrt{\frac{\pi}{\mu}}\exp\{\nu^2/\mu\}\{1-\mathrm{erf}(\frac{\nu}{\sqrt{\mu}})\}+\\ \frac{1}{2\mu}+\frac{\nu}{2\mu}\sqrt{\frac{\pi}{\mu}}\exp\{\nu^2/\mu\}\{1-\mathrm{erf}(\frac{-\nu}{\sqrt{\mu}})\}\end{array}\right], \tag{A.7}$$

where $\mathrm{erf}(\cdot)$ is the error function and $\beta^2=b^2+a^2/\sigma^2=\mathbf{m}^{\mathrm{T}}\boldsymbol{\Sigma}^{-1}\mathbf{m}$. Recalling that $\mathrm{erf}(\cdot)=\mathrm{erf}(-)$, (A.7) can be rewritten as:

$$p_z(z)=\frac{\exp\{-\beta^2 2\}}{2\pi|\Sigma|^{1/2}}\left[1+\sqrt{\frac{\pi\nu^2}{\mu}}\exp\{\nu^2\mu\}\mathrm{erf}\left(\frac{\nu}{\sqrt{\mu}}\right)\right]. \tag{A.8}$$

References

[1] C. Li, T.W. Chou, Phys. Rev. B 68 (2003) 073405.
[2] B. Ilic, D. Czaplewski, H.G. Craighead, P. Neuzil, C. Campagnolo, C. Batt, Appl. Phys. Lett. 77 (2000) 450.
[3] K. Jensen, C. Girit, W. Mickelson, A. Zettl, Phys. Rev. Lett. 96 (2006) 215503.
[4] C. Li, T.W. Chou, Appl. Phys. Lett. 84 (25) (2004) 5246.
[5] J.P. Salvetat, J.A.D. Briggs, J.M. Bonard, R.R. Bacsa, A.J. Kulik, T. Stöckli, N.A. Burnham, L. Forró, Phys. Rev. Lett. 82 (5) (1999) 944.
[6] A. Krishnan, E. Dujardin, T.W. Ebbesen, P.N. Yianilos, M.M.J. Treacy, Phys. Rev. B 58 (20) (1998) 14013.
[7] R. Gao, Z.L. Wang, Z. Bai, W. de Heer, L. Dai, G. Mei, Phys. Rev. Lett. 85 (3) (2000) 622.
[8] J.Z. Liu, Q. Zheng, Q. Jiang, Phys. Rev. B 67 (2003) 075414.
[9] T.S. Gates, G.M. Odegard, S.J.V. Frankland, T.M. Clancy, Compos. Sci. Technol. 65 (2005) 2416.
[10] Y. Huang, J. Wu, K.C. Kwang, Phys. Rev. B 74 (2006) 245413.
[11] A.V. Barzykin, M. Tachiya, Phys. Rev. B 72 (2005) 075425.
[12] I.Y. Lee, X. Liu, B. Kosko, C. Zhou, Nano Letters 3 (12) (2003) 1683.
[13] D. Blevins, Formulas for Natural Frequencies and Vibration, Van Nostrand, New York, 1978.

[14] K.I. Tserpes, P. Papanikos, Composites B 36 (2005) 468.
[15] A. Papoulis, S.U. Pillai, Probability, Random Variables and Stochastic Processes, 4th Ed., McGraw-Hill, Boston, USA, 2002.
[16] ANSYS, 10.0 Users' Manual, Swanson Inc., 2005.
[17] G.M. Odergard, T.S. Gates, L.M. Nicholson, K. Wise, Compos. Sci. Technol. 62 (2002) 1868.
[18] W.D. Cornell, P. Cieplak, C.I. Baily, I.R. Gould, K.M. Merz, D.M. Ferguson, et al.J. Am. Chem. Soc. 17 (1995) 5179.
[19] W.C. Young, Roark's Formulas for Stress and Strain, 6th International Ed., McGraw-Hill, 1989.
[20] S.T. Purcell, P. Vincent, C. Journet, V.T. Binh, Phys. Rev. Lett. 89 (27) (2002) 276103.
[21] J.P. Lu, Phys. Rev. Lett. 79 (1997) 1297.
[22] E. Hernández, C. Goze, P. Bernier, A. Rubio, Phys. Rev. Lett. 80 (1998) 4502.
[23] C. Li, T.W. Chou, Int. J. Solids Struct. 40 (2003) 2487.
[24] Y. Jin, F.G. Yuane, Compos. Sci. Technol. 63 (2003) 1507.
[25] H.J. Qi, K.B.K. Teo, K.K.S. Lau, M.C. Boyce, W.I. Milne, J. Robertson, K.K. Gleason, J. Mech. Phys. Solids 51 (2003) 2213.
[26] K.F. Graff, Wave Motion in Elastic Solids, Dover Publications, Inc., New York, 1991.